A closed-loop design methodology for underwater transducers pulse-shaping

Marco Morgado, Paulo Oliveira, and Carlos Silvestre

***Abstract*— This paper presents a novel methodology for signal generation with application to underwater ranging systems. The proposed technique resorts to a closed loop output voltage feedback, optimal control strategy that modifies the acoustic signals transmitted by the underwater transducers, aiming to improve the detection. Given the signals selected *a priori*, the design of the pulse-shaping equalizer is further modified to consider a preview term associated with the reference signals available. The performance of this enhancement methodology is assessed from the results obtained with realistic simulations and through the analysis of experimental data acquired in sea trials.**

I. Introduction

A vast number of underwater applications rely on the precise ranging information to reference points. The successful execution of these tasks, that include environmental monitoring, surveillance, underwater inspection of estuaries, harbors, and pipelines, and geological and biological surveys, requires low-cost, compact, high performance, and robust navigation systems that can accurately estimate the underwater vehicles position and attitude. Out of several key issues on the design and implementation of underwater ranging systems, the selection of appropriate signals and their accurate generation plays a major role on the improvement of the resolution and precision of range measurements. This paper presents a novel pulse-shaping emission filters design approach, resorting to optimal feedback control techniques, to improve the ranging precision of underwater positioning systems with transducers.

On a general overview, the design of precise underwater ranging systems often includes three major aspects: i) the design of advanced signals that dramatically improves the detection Signal to Noise Ratio (SNR), such as Direct Spread-Spectrum Signals (DSSS) [1], that allows for improved precision, robustness to ambient or jamming noise, increased update rate, and simultaneous multi-user capabilities, as opposed to conventional signals like sinusoidal pulses and chirp tone bursts; ii) the development of advanced algorithms on the reception for improved detection and equalization via channel impulse response estimation and other techniques, see[2] and references therein; and iii) the performance enhancements provided by the previous approaches, are not deliverable to their full capabilities if the underwater acoustic transducers frequency response, limitations, and non-linearities are not properly taken into account on the emission side. If when operating as hydrophones (listening state) underwater transducers have a fairly flat broadband amplitude/phase frequency response, when being excited to generate acoustic pressure waves, underwater transducers rather have a narrower transmitting bandwidth (and with limitations on the input voltage, which should not be neglected). Closely related work for pulse-shaping and transfer function equalization can be found in [3], [4] in which the design of inverse Finite Impulse Response (FIR) filters for the transducers has been considered. Other approaches include the employment of Weighted Least Squares (WLS) pulse-shaping techniques to improve the matched-filter output peak detection and time-resolution, and the integrated approach design [5], as opposed to buying commercially available transducers and interfacing them with adapted matching networks. The design of complex broadband matching networks with Lumped elements has also been addressed [6], although the design and implementation of such networks can be quite complex. The demand for low-cost, small and compact matching circuits / pulse shaping filters is increasing with the need of compact and power efficient vehicles and navigation systems. To the best knowledge of the authors, the explicit inclusion of input voltage limitations has not been addressed in the previous approaches. This paper focuses on the improvement of the range measurements by taking into account the dynamical characteristics and limitations of the transducers on the emission of the underwater signals. The optimal control method proposed in this paper allows for the natural and explicit inclusion of input voltage limitations on the equalization of the emission transducer and amplifier. The proposed technique fully exploits the information provided by the reference signal to be emitted, which is known *a priori*, as a preview input for the control system allowing for a significant improvement on the response of the overall system. The performance of the proposed technique is assessed from simulations results and is also validated from the analysis of experimental data from sea trials.

The paper is organized as follows: the design of the pulse-shaping filter, together with the inclusion of the preview information on an optimal control problem, is brought to full detail in Section II. An application example to a realistic underwater transducer model is detailed in Section III, where realistic simulation results validate the equalization performance. The implementation of the proposed architecture is validated with experimental results at sea in Section III-B, and finally Section IV provides some conclusion remarks and comments on future work.

II. Pulse-shaping filter design

The design of any underwater acoustic ranging system, requires a measurement of the Time-Of-Flight (TOF) of a signal. As for any coherent detection problem, a TOF good estimate may be obtained by passing the input signal

This work was partially supported by Fundação para a Ciência e a Tecnologia (ISR/IST plurianual funding), by the project FCT PTDC/EEA-CRO/111197/2009 - MAST/AM of the FCT, and by the EU Project TRIDENT (Contract No. 248497). The work of Marco Morgado was supported by PhD Student Scholarship SFRH/BD/25368/2005 from the Portuguese FCT POCTI programme.

The authors are with the Institute for Systems and Robotics, Instituto Superior Técnico, Av. Rovisco Pais, 1, 1049-001, Lisbon, Portugal {marcomorgado,pjcro,cjs}@isr.ist.utl.pt

through a matched-filter whose impulse response is a time-reversed replica of the expected signal. In ideal conditions, the filter output is related to the autocorrelation function of the received signal. Specially designed spread-spectrum modulated signals have known good autocorrelation properties [7] allowing for a narrower output peak of the matched-filter and improving the performance of the detector. Affected by unequalized distortions and in non-ideal conditions, the output peak of the matched-filters spread in time, degrading the performance of such detectors.

Consider an underwater transducer with an equivalent admittance $Y(s)$ given by (see [8] for the evaluation of underwater transducers equivalent circuits)

$$Y(s) = {}^{I(s)}/_{V_o(s)} = G + jB = Z^{-1}(s)$$

where $Z(s)$ is the impedance, G the conductance, B the susceptance, I the input current, and V_o is the voltage at the electric terminals of the acoustic transducer.

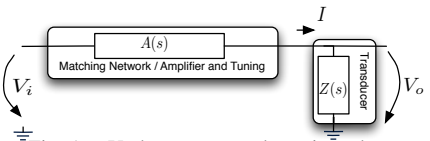

Fig. 1. Underwater transducer impedance

In order to obtain a voltage controlled device when designing a matching network or pulse-shaping filter, a power amplifier denoted as $A(s)$ is used as shown in Fig. 1. Instead of designing complex matching networks for $A(s)$, such that Input-to-Output transfer function $H(s) = {}^{V_i}/_{V_o}$ becomes $H(s) \approx \mathbf{I}$, a simpler, lower cost, efficient power amplifier (i.e. a Class D PWM - Pulse Width Modulated switching power amplifier) or simpler narrowband tuning (i.e. a single resonator) could be devised as in the amplifier and pulse-shaping filter $G(s)$ illustrated in Fig. 2.

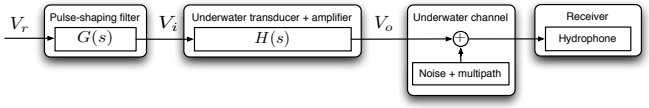

Fig. 2. Transducer and pulse-shaping filter

From the available techniques [3], [2], [4], [5], [6] that can be employed to improve the detection of the signal V_r on the receiving entity in Fig. 2, given the disturbances present in the underwater channel, this paper focuses on improving this detection by actuating merely on the transmission signal conditioning. Ideally, a typical design criteria for this type of systems is the time-resolution of the matched-filters outputs at the reception: narrower matched-filter output main lobe results in improved detection.

A. Deconvolution problem

The pulse-shaping design problem considered herein can be related to the deconvolution of a single channel system where an inverse FIR filter is designed to equalize the transducer transfer function [3], [2]. Considering $G(z)$ and $H(z)$ to be the z-transform (equivalent in the discrete domain) of $G(s)$ and $H(s)$, respectively, in Fig. 2, the design of an approximate inverse FIR of the transducer involves minimizing a frequency-dependant cost function of the type [3]

$$J(z) = E^H(z)E(z) + \beta B^H(z)B(z) \tag{1}$$

where the term $E^H(z)E(z)$ is a quadratic error term associated to the output performance error that measures how well the desired reference signal V_r is reproduced at the output V_o, the term $\beta B^H(z)B(z)$ is called the regularization term that penalizes the amount of energy spent on the generation of the input signal V_i, and the superscript H denotes the usual Hermitian operator.

The regularization term can conveniently be used to suppress or to boost certain frequency regions of the transducer frequency response, and to limit the use of high amplitudes on the input signal V_i. By varying β from zero to infinity, one can gradually shape the solution to minimize solely the performance error to minimizing only the energy input. The filter that represents the optimal solution, in a least-squares sense, to the cost function (1) is given by [3], [2]

$$G(z) = \frac{H(z^{-1})}{H(z^{-1})H(z) + \beta B(z^{-1})B(z)}.$$

from which the optimal signal V_i is obtained by filtering the desired signal V_r. As carefully argued in [3], the choice of the exact value of β is not critical although it demands some care and is rather subjective based on the resulting performance of the deconvolution and the required amplitude (or energy) of the filtered input signal to the transducers.

B. Preview Linear Quadratic Regulator pulse-shaping filter

Suppose that the transfer function of the voltage controlled system composed by the transducer and the simple amplifier and narrowband tuning circuitry $H(s)$ has a discrete state space realization given by

$$\begin{cases} x(k+1) = Ax(k) + Bu(k) \\ V_o = Cx(k) \end{cases} \tag{2}$$

where $x(k) \in \mathbb{R}^n$ is the system state, of dimension n, $u(k) = V_i(kT_s)$ is the input voltage sampled at the time instants $t_s = kT_s$ with $k = 1, 2, \ldots$ and T_s is the sampling period of the system.

The novel design methodology proposed in this paper is inherited directly from the design of a Discrete Linear Quadratic Regulator (DLQR) [9], [10] in a closed loop configuration as illustrated in Fig. 3. The infinite horizon Linear Quadratic Regulation (LQR) problem is an optimal control strategy that yields a state feedback law that minimizes an error and control energy based quadratic cost function. In particular, it computes a matrix gain K such that the state-feedback control law

$$u(k) = -Kx(k) \tag{3}$$

stabilizes the resulting closed-loop system when applied to (2).

Interestingly enough, if the pair (A, B) is stabilizable, the solution for $u(k)$ in (3) is unique and the resulting closed-loop controller is stable [10]. Thus, the feedback of the voltage at the transducer terminals and the modelled discrete states allows for an identification of the pulse-shaping filter in a straightforward manner based on a dynamical

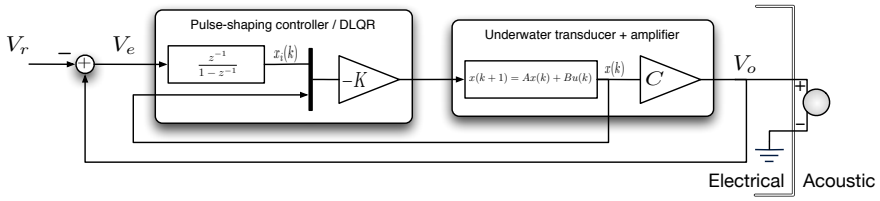

Fig. 3. Pulse-shaping filter controller with augmented integral state

model of underwater transducer and power amplifier. The reasoning for placing a DLQR in the loop as shown in Fig. 3 is justified from the fact that if $V_r = 0$, the DLQR asymptotically stabilizes the solution of the discrete state $x(k)$ to a constant value and consequently drives the voltage error $V_e = V_o - V_r$ to zero. This convergence is ensured by the augmented discrete integrator of the voltage error by stabilizing $x_i(k)$ to a constant value and consequently the input of the discrete integrator V_e to zero. Assuming that the closed-loop bandwidth of the system is much greater than the frequency of V_r, the controlled pulse-shaping filter will force the output V_o to track the reference signal V_r.

The computation of the gain K for the augmented integral state system in Fig. 3 is accomplished by computing the DLQR gain for the equivalent augmented system

$$\begin{cases} \bar{x}(k+1) = \bar{A}\bar{x}(k) + \bar{B}u(k) + \bar{L}V_r(k) \\ V_o = \bar{C}\bar{x}(k) \end{cases},$$

where

$$\bar{x}(k) = \begin{bmatrix} x^T(k) & x_i(k) \end{bmatrix}^T,$$

$$\bar{A} = \begin{bmatrix} A & 0 \\ C & 1 \end{bmatrix}, \bar{B} = \begin{bmatrix} B \\ 0 \end{bmatrix}, \bar{L} = \begin{bmatrix} \mathbf{0} & -1 \end{bmatrix}^T, \bar{C} = \begin{bmatrix} C & 0 \end{bmatrix},$$

and making $u(k) = -K\bar{x}(k)$.

Given that the reference signal to be emitted is known *a priori*, the controller can benefit from future information about the reference signal in order to improve its performance. The idea of placing an active dynamical system to control the output of the filter is not novel, it has been patented in [11], and a similar approach to dynamically controlled matching network design can be found in [12]. Nonetheless, the application of preview information from the reference signal to pulse-shaping filter design is new. Preview information has been previously applied to control problems in [13] for active suspension design by road preview and in [14] for vehicle lateral guidance in automated highways . For the preview information to be valid and modelled as a First-In-First-Out (FIFO) pipeline and the overall solution to be optimal, in [14] it was assumed that during the preview horizon no external input (e.g. the driver turning the wheel) could change the preview information. This is not the case of the work presented herein since the reference signal that is to be transmitted is already known *a priori*, which fits naturally in the preview control framework. For thorough details on preview control, the readers are directed to previous work in [14] and references therein.

Thus, the preview information from the reference signal is modelled as a FIFO buffer and introduced in the overall system model using the additional dynamical system

$$\begin{cases} x_p(k+1) = Dx_p(k) + Ep_o(k) \\ s(k) = Hx_p(k) \end{cases},$$

where $p_o(k) = V_r(k+p+1)$ is the output of the sample reference signal previewer at the time instant $t((k+p+1)T_S)$, p is the preview horizon,

$$E = \begin{bmatrix} \mathbf{0} & \cdots & \mathbf{0} & \mathbf{I} \end{bmatrix}^T, \qquad H = \begin{bmatrix} 0 & \mathbf{0} \\ -1 & \mathbf{0} \end{bmatrix},$$

and $D = \{D \in \mathbb{R}^{p\times p} : D_{ij} = 1 \text{ if } j = i+1, 2 \le i \le p,\ D_{ij} = 0 \text{ otherwise}\}$ ensembles the FIFO delay line.

Sustained on the D-methodology introduced in [15], the trapezoidal discrete integrator, shown if Fig. 3 is detached from the unit delay and placed in front of the gain $-\bar{K}$ as a backward Euler integrator. The voltage limitation is thus easily implemented using the integral saturation u_{MAX} as shown in Fig. 4. This value is set such that it complies with the voltage limitations at the input stage of the combined amplifier and transducer system.

The computation of the augmented gain $\bar{K}$ is accomplished by designing the DLQR for the equivalent system with the augmented structure that accounts for the feed-forward preview information

$$\begin{cases} \bar{\bar{x}}(k+1) = \begin{bmatrix} \bar{A} & H \\ \mathbf{0} & D \end{bmatrix} \bar{\bar{x}}(k) + \begin{bmatrix} \bar{B} \\ \mathbf{0} \end{bmatrix} u(k) + \begin{bmatrix} \mathbf{0} \\ E \end{bmatrix} p_o(k) \\ V_o = \begin{bmatrix} \bar{C} & \mathbf{0} \end{bmatrix} \bar{\bar{x}}(k) \end{cases}$$

where $\bar{\bar{x}}(k) = \begin{bmatrix} x^T(k) & x_i(k) & x_p^T(k) \end{bmatrix}^T$.

III. Application Example

The presented pulse-shaping methodology is exemplified in this section using numerical simulation results and experimental results with an underwater acoustic transducer. For demonstration purposes, a broadband single resonant frequency ($79\,KHz$) spherical omnidirectional transducer ITC-1042 was considered and for the sake of simplicity the transducer is considered to be modelled by an equivalent impedance with a resistor and a capacitor, with a simple single resonance tuning circuit based on a power amplifier stage, a resonator and a resistor, as shown in Fig. 5(a). Simulation results using this simple model are presented in Section III-A where the performance enhancement on the time-resolution of the matched-filter output is evidenced when compared to the unequalized signal. The proposed technique is further validated in a experimental setting with tests at sea and results presented in Section III-B. A Binary Phase Shift Keying (BPSK) modulated DSSS signal is used which phase changes are synchronized with the voltage signal shift to avoid energy disruptions and discontinuities

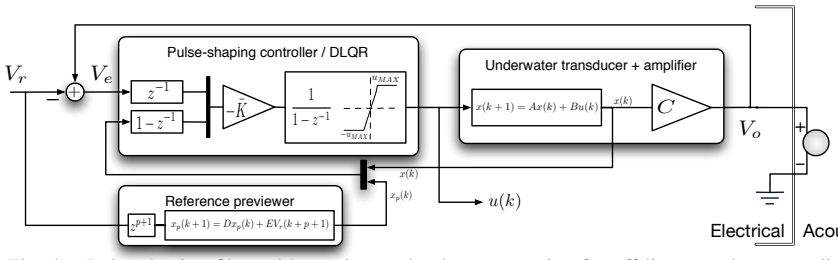

Fig. 4. Pulse-shaping filter with preview and voltage saturation for off-line transducer equalization

at the terminals of the transducer. To generated the DSSS signal, a 127 chips Gold Code was used to BPSK modulate a 25 KHz carrier sinusoid, with a chip rate equal to one full period of the carrier, spanning 5.08 ms in time.

A. Simulation results

For tuning purposes, and based on Fig. 5 the following relation is easily established for the transducer water impedance

$$Z_{eq}(s) = Y_{eq}^{-1}(s) = {}^{G}/_{(G^2+B^2)} + j{}^{-B}/_{(G^2+B^2)}$$

The equivalent transfer function $H(s)$ can be written as

$$H(s) = {}^{V_o(s)}/_{V_i(s)} = {}^{Z_{eq}(s)}/_{(Z_{eq}(s)+Z_{tn}(s))},$$

where the denominator of $H(s)$ is given by $s^2 + {}^{(R_{eq}+R_{tn})}/_{L_{tn}}s + {}^{1}/_{(L_{tn}C_{eq})}$. Comparing the denominator of $H(s)$ with the denominator of traditional design low-pass like filters $d(s) = s^2 + 2\xi s + \omega_0^2$, where the tunable parameters ω_0 and ξ represent respectively the filter resonant frequency and its bandwidth, allows to tune L_{tn} and R_{tn} to the desired frequency and bandwidth, within reasonable values. Thus, L_{tn} is selected to yield an approximate resonant frequency of $25KHz$, with $L_{tn} = {}^{1}/_{(\omega_0^2 C_{eq})} = {}^{1}/_{(4\pi^2 f_0^2 C_{eq})}$, where f_0 is the resulting resonant frequency in Hz and C_{eq} is evaluated from the transducer admittance calibration data at $\omega = 2\pi f_0$. In order to yield the desired bandwidth the tuning resistance R_{tn} should be selected using the bandwidth parameter $\Delta f = {}^{\Delta\omega}/_{2\pi} = {}^{\xi}/_{\pi} = {}^{(R_{eq}+R_{tn})}/_{(2\pi L_{tn})}$. However, as claimed in [11], the resistor R_{tn} should not be very large to avoid transmission power losses by heat, and thus in the proposed technique, R_{tn} is solely considered to be the electrical and electronic wiring resistance (negligible when compared to R_{eq}).

Thus, a simple resonant tuning using a single solenoid was considered, yielding a very narrow band transfer function as shown in the Bode magnitude diagram in Fig. 5(c), and further emphasizes the application of the proposed technique to low cost tuning circuits. This type of tuning is typically used to transmit narrow frequency pulses such as pure tone sinusoidal pulses. A perturbed plant is also considered to evaluate the proposed technique, which results from changing by 5% the tuning coil value, the gain and the fastest pole and zero of the transducer transfer function.

The transducer transfer function was identified using system identification techniques and tools from MATLAB ARX system identification toolbox, and from the manufacturer specifications and calibration data sheet, see Fig. 5(b), and

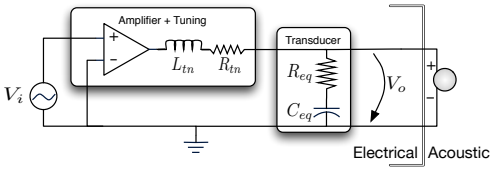

(a) Transducer model

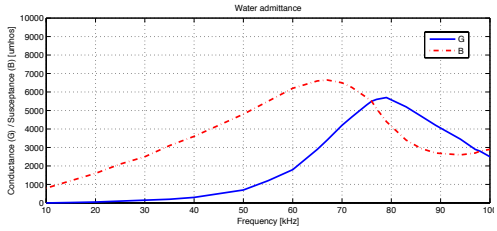

(b) ITC-1042 admittance

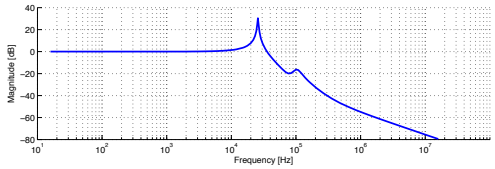

(c) $H(s)$ magnitude Bode diagram

Fig. 5. Underwater transducer model application example

is given by $H(s) = k\prod_{i=1}^{8}(s-z_i)/\prod_{i=1}^{9}(s-p_i)$, where

$$k = 10564.94,\ \begin{bmatrix} p_1 \\ \vdots \\ p_9 \end{bmatrix} = \begin{bmatrix} -6.6763\times10^5 \\ -6.5082\times10^5 \\ (-1.0198+j6.3848)\times10^5 \\ (-1.0198-j6.3848)\times10^5 \\ (-1.0717+j6.2865)\times10^5 \\ (-1.0717-j6.2865)\times10^5 \\ (-0.0233+j1.6208)\times10^5 \\ (-0.0233-j1.6208)\times10^5 \\ -533.5852 \end{bmatrix},\ \begin{bmatrix} z_1 \\ \vdots \\ z_8 \end{bmatrix} = \begin{bmatrix} -20.000\times10^5 \\ -13.581\times10^5 \\ -6.508\times10^5 \\ (-1.072+j6.286)\times10^5 \\ (-1.072-j6.286)\times10^5 \\ (-1.160+j4.921)\times10^5 \\ (-1.160-j4.921)\times10^5 \\ -533.5852 \end{bmatrix}.$$

For technique comparison purposes, an asymmetric inverse FIR pulse-shaping filter was also considered in the simulation results allowing to evaluate the proposed architecture with more traditional solutions, as presented in Section 1. Both classical unregulated inverse FIR with $\beta = 0$ and a state-of-the-art regulated inverse FIR were considered. The regularisation term was design in frequency to shape $20\,dB$ on the frequency band $20 - 40\,KHz$, while damping the remaining bands to $0\,dB$, and with $\beta = 1$. The length of the FIR filters are considered to be of the same size as the input signal. The filters are also evaluated using a performance metric based on the inverse of the filter output energy on a window around its peak. Thus, the decibel (dB) values represented in the

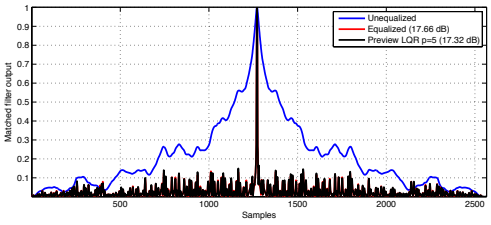

Fig. 6. Output signal autocorrelation

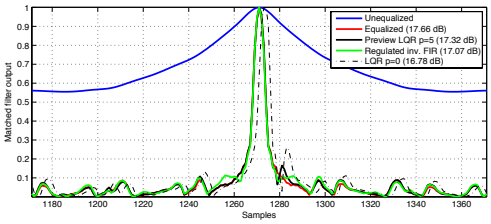

Fig. 7. Output signal autocorrelation zoom with regulated inverse FIR

following Figures are based on the improvement provided by the filters compared to the unequalized output.

As expected, the time-resolution improvement from the unequalized to the equalized case, is evidenced from the results presented in Fig. 6, where the output of the matched-filter is plotted for the unequalized signal, for the perfectly equalized signal, and finally for the Preview LQR equalized signal using the technique presented herein with a preview horizon of 5 samples. The same matched filter output is zoomed in Fig. 7 around its peak, where the matched filter output of the LQR without preview and of the regulated inverse FIR are also shown. As it can be seen, the proposed technique is able to achieve the same narrow matched-filter output peak of the perfectly equalized signal, and of the regulated inverse FIR. On the other hand, the output of the matched filter for the LQR without preview equalization evidences a clear offset from the nominal peak.

When considering the classical unregulated inverse FIR equalization, the transducer excitation signal required by each approach to yield the same signal output level is plotted in Fig. 8 where it can be seen that the inverse FIR design clearly surpasses the input voltage limitation of the transducer. As a result, the corresponding excitation signal needs to be scaled to avoid the input signal to exceed its voltage limitations. Naturally, this scaling reflects itself on the output signal level being much lower than expected as demonstrated in Fig. 9. The signal generated by the Preview LQR is shown to correctly follow the reference signal, while the LQR without preview information evidences a significant phase delay and is not able to track the reference signal as desired. The same comparison analysis is conducted for the regulated inverse FIR equalization in Fig. 10 with its output plotted in Fig. 11. Even though the regularisation term allows for the input effort to be penalized resulting in a lower amplitude input signal, the input voltage limitation is not explicitly employed. Moreover, the LQR with preview equalization evidences better reference signal tracking in Fig. 11.

B. Experimental results

Preliminary experimental trials were conducted in a harbor, in Sesimbra - Portugal, to assess the feasibility of the

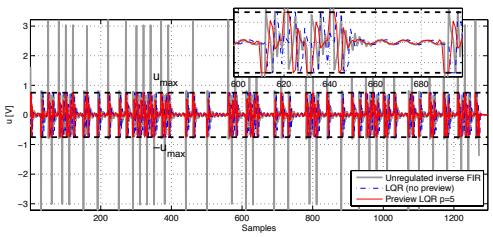

Fig. 8. Transducer excitation signal with unregulated inverse FIR

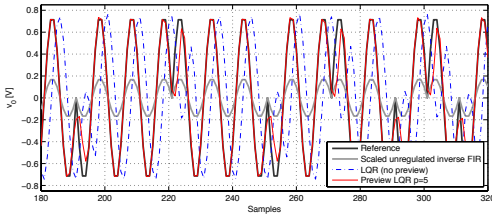

Fig. 9. Unregulated inverse FIR Equalized transducer voltage (zoom)

acoustic ranging system. In these tests, two hydrophones, placed 20 *cm* apart, were fixed to the pier at about 2.5 *m* deep. The transmitter, also submerged around 2.5 *m* on each transmission location, was placed in several locations in the field of view of the receiving hydrophones so that several distances and SNR scenarios could be emulated. The underwater sound speed was about 1514 ms^{-1} as measured by a Sound Velocity Profiler (SVP). An aerial view of Sesimbra Marina is depicted in Fig. 13(a), where the receiving array position and the transmitter locations are illustrated. Several boats were floating inside the marina besides the floating piers, and combined with a maximum depth of 9 meters, the test conditions were not ideal. In fact rather harsh and quite far from ideal, which further strengthens the results obtained. The transmission and reception were performed using the prototype hardware developed in-house and depicted in Fig. 12, and synchronized with the GPS 1-PPS clock with a precision of 1 μs. The signals were generated using a Class D PWM power amplifier, and recorded underwater for post processing using the reception amplifiers set to a fixed gain. From each of the 7 transmitting locations, 8 copies of the signals were recorded for post processing.

The matched-filters outputs from the experimental results

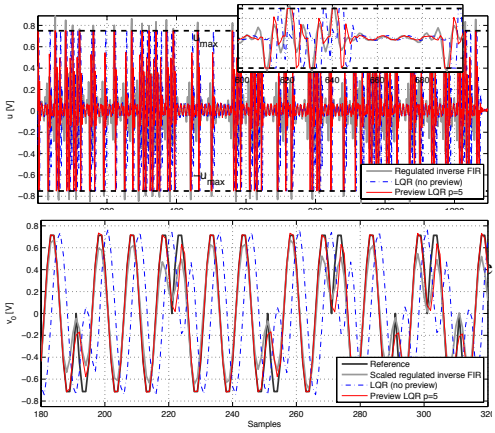

Fig. 11. Regulated inverse FIR Equalized transducer voltage (zoom)

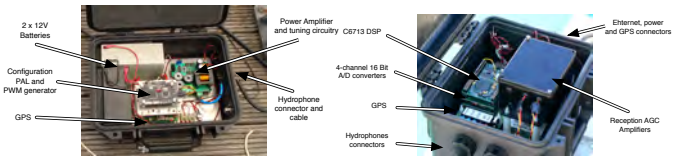

(a) Emission splash-proof box (b) Reception splash-proof box

Fig. 12. Prototype systems for sea trials

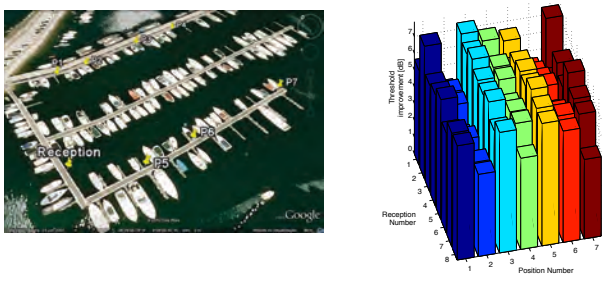

(a) Harbor test site (b) Threshold improvement

Fig. 13. Experimental trials: (a) harbor test site and (b) threshold improvement between unequalized signal and LQR with preview equalized

are plotted in Fig. 14, which experimentally evidences the performance enhancement of the proposed technique. The average improvement using the before-mentioned performance metric tops out at around 6.22 dB as opposed to the 17.32 dB enhancement from the simulation results. The threshold improvement is better illustrated for all the transmissions in Fig. 13(b) in which the improvement is shown to be quite uniform from all the positions. The narrow peak obtained experimentally can be better evaluated in Fig. 15 from one of the receptions obtained in position P4.

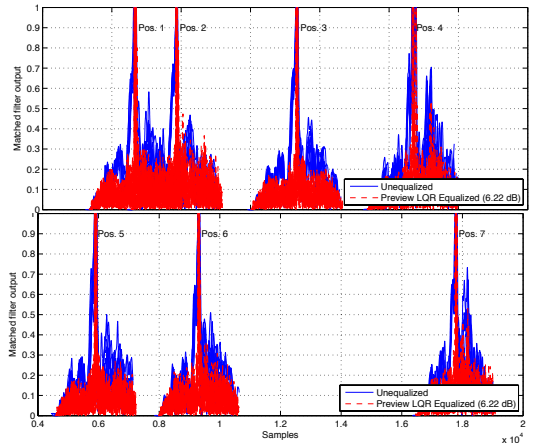

Fig. 14. Experimental matched filter output envelopes

IV. Conclusions

This paper presented a novel methodology for the design and implementation of transmission pulse-shaping filters. The proposed technique is based on closed-loop control strategies with preview information and is shown to be able to improve the detection of the transmitted signals by directly modifying the transmission pulse-shaping filters. The

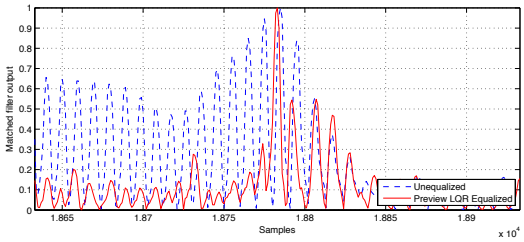

Fig. 15. Experimental matched filter output envelope for reception position P4

performance enhancement was evident from the presented simulation results and was validated using real data from experimental sea trials. The closed-loop preview control technique that was proposed also offers other advantages: voltage limitations on the underwater transducer are introduced in feedback loop, and can be implemented using state-of-the-art digital microprocessing systems with low-cost, compact and power efficient amplifiers as opposed to bulky and complex power amplifying systems. Moreover, if the signals are not equalized by the transmitting entities for their own transducers distortions the receiving agents need to have further knowledge of the transmitting transducers transfer functions (in fact, one calibrated transfer function for each transmitting agent). The architecture presented herein allows for the creation of a large code-book of signals that could be stored on memory of the transmitting devices, or it can be used for on-line transducer equalization with a state observer employed in the feedback loop.

References

[1] B. Bingham, B. Blair, and D. Mindell, "On the design of direct sequence spread-spectrum signaling for range estimation," in *OCEANS 2007*, 2007, pp. 1–7.

[2] L. Freitag, M. Stojanovic, S. Singh, and M. Johnson, "Analysis of channel effects on direct-sequence and frequency-hopped spread-spectrum acoustic communication," *IEEE Journal of Oceanic Engineering*, vol. 26, no. 4, pp. 586–593, 2001.

[3] O. Kirkeby, P.A. Nelson, H. Hamada, and F. Orduna-Bustamante, "Fast deconvolution of multichannel systems using regularization," *Speech and Audio Processing, IEEE Transactions on*, vol. 6, no. 2, pp. 189 –194, Mar. 1998.

[4] O. Kirkeby, P. Rubak, and A. Farina, "Analysis of ill-conditioning of multi-channel deconvolution problems," in *1999 IEEE Workshop on Applications of Signal Processing to Audio and Acoustics-Mohonk Mountain House New Paltz, New York October*. IEEE, 1999, pp. 17–20.

[5] R.F.W. Coates, "The design of transducers and arrays for underwater datatransmission," *IEEE Journal of Oceanic Engineering*, vol. 16, no. 1, pp. 123–135, 1991.

[6] B.S. Yarman, M. Sengul, and A. Kilinc, "Design of practical matching networks with lumped elements via modeling," *IEEE Transactions on Circuits and Systems I: Regular Papers*, vol. 54, no. 8, pp. 1829–1837, 2007.

[7] D. V. Sarwate and M. B. Pursley, "Crosscorrelation properties of pseudorandom and related sequences," 1980, vol. 68, pp. 593–619.

[8] R. Ramesh and D. Ebenezer, "Equivalent circuit for broadband underwater transducers," *IEEE Transactions on Ultrasonics, Ferroelectrics and Frequency Control*, vol. 55, no. 9, pp. 2079–2083, 2008.

[9] G.F. Franklin, J.D. Powell, and M.L. Workman, *Digital Control of Dynamic Systems*, Addison-Wesley, 1980.

[10] K. Zhou, J.C. Doyle, and K. Glover, *Robust and optimal control*, Prentice Hall Englewood Cliffs, NJ, 1995.

[11] DOUST and P. Edwin, "Method and apparatus for equalising transfer functions of linear electro-acoustic systems," Patent Application, 11 2001, WO 2001/083122 A1.

[12] J.S. Fu and A. Mortazawi, "Improving power amplifier efficiency and linearity using a dynamically controlled tunable matching network," *Microwave Theory and Techniques, IEEE Transactions on*, vol. 56, no. 12, pp. 3239–3244, 2008.

[13] M. Tomizuka, "Optimum Linear Preview Control With Application to Vehicle Suspension," *Journal of Dynamic Systems, Measurement, and Control*, vol. 98, pp. 309, 1976.

[14] H. Peng and M. Tomizuka, "Preview control for vehicle lateral guidance in highway automation," *Journal of Dynamic Systems, Measurement, and Control*, vol. 115, pp. 679, 1993.

[15] I. Kaminer, A. Pascoal, P. Khargonekar, and E. Coleman, "A velocity algorithm for the implementation of gain-scheduled controllers," *Automatica*, vol. 31, no. 8, pp. 1185 – 1191, 1995.

[16] R.G. Brown and P.Y.C. Hwang, *Introduction to Random Signals and Applied Kalman Filtering*, John Wiley & Sons, third edition, 1997.